Proceedings of the 21st ICSMGE, Vienna, Austria, 14 – 19 June 2026. Pistrol, Adam & Schweiger (eds.)
Published by: ÖGG, Austrian Society for Geomechanics, Salzburg, Austria, ISBN 978-3-9503898-4-5
https://doi.org/10.53243/ICSMGE2026-2225

Effect of Groundwater-Induced Heat Convection on Energy Wall Systems: A 3D Numerical Modeling Approach

Ba Huu Dinh
Basic Research Laboratory (BRL), Chonnam National University, Gwangju, Republic of Korea

Wonjun Choi
School of Architecture, Chonnam National University, Gwangju, Republic of Korea

Jaehong Kim
Department of Civil Engineering, Dongshin University, Naju, Republic of Korea

Young-Sang Kim
Department of Civil Engineering, Chonnam National University, Gwangju, Republic of Korea, geoyskim@jnu.ac.kr

ABSTRACT: Thermally induced groundwater flow may have a significant influence on the heat transfer performance and the soil temperature during the operation of an energy wall system (EWS). However, few studies quantitatively evaluate the influence of heat convection induced by groundwater flow on the heat transfer performance of an EWS (i.e., outlet fluid temperature (°C), and heat exchange rate (W)). This study evaluated the influence of three different types of heat convection (natural, forced, and mixed convection regimes) induced by groundwater (GW) low on the heat transfer performance of an EWS by a numerical simulation. A finite element method-based 3D numerical model was employed to simulate the actual dimension of a subway station constructed in Gwangju, South Korea. The model was validated with the in situ thermal response test with a steel U-type heat exchanger embedded in a concrete volume of 2 × 3 × 5 m (width × depth × length). The results indicated that natural convection was dominant at a groundwater velocity below10^{-7} m/s, while forced convection was dominant at a velocity above 5×10^{-6} m/s. Between these ranges of groundwater velocity, mixed convection (the combination of forced and natural convection) was observed. For the summer season, the thermally induced groundwater flow resulted in reducing the outlet fluid temperature of 8 °C, 11 °C, and 15 °C for natural convection, mixed convection, and forced convection compared to that of only heat conduction, respectively. Consequently, the heat exchange rate of EWS was enhanced by 41.5%, 56.8%, and 73.1%, respectively. These findings suggest that neglecting thermally induced groundwater flow may significantly underestimate the thermal performance.

KEYWORDS: Energy Geostructure, energy wall, thermally induced groundwater flow, geothermal energy, heat transfer performance.

1 INTRODUCTION

Using clean, renewable and sustainable energy sources to replace fossil fuels and natural energy is one of the most effective solutions to achieve the goal of net zero emissions by 2050. Energy used for buildings accounts for the largest part of the world's energy consumption. In recent years, geothermal systems have been widely studied and used in heating/cooling buildings (Sarbu and Sebarchievici, 2014). This system takes advantage of the stability of underground temperatures as an energy reserve (Gao et al., 2021). Compared to traditional air source heat exchange systems, this system has many advantages, such as being environmentally friendly, saving fuel, and reducing carbon emissions (Kim et al., 2012).

Energy walls are mostly installed below the water table; therefore, the water flow affects the operation of this system. In recent years, there have been many studies on the effects of groundwater convection, natural convection on the temperature of the surrounding soil, and the performance of geothermal energy systems. Natural convection is created by buoyancy, which occurs when the density of water is changed due to the temperature change caused by the operation of EWS. Typical studies related to natural convection are as follows: (Zhao et al., 2008; Sharqawy, Badr and Mokheimer, 2013; Spitler, Javed and Ramstad, 2016; Javed and Spitler, 2017; Ghasemi-Fare and Basu, 2018; 2019; Tamizdoust and Ghasemi-Fare, 2020; Bidarmaghz and Narsilio, 2022; Najafian Jazi, Ghasemi-Fare and Rockaway, 2024). Spitler et al. (2016) conducted a U-type TRT in a groundwater-filled borehole to evaluate the effect of natural convection on the thermal resistance of the boreholes. They found that the effect of the natural convection strongly depends on the heat transfer rate and annulus temperature. Ghasemi-Fare and Basu (2018) performed the mockup TRT in laboratory for saturated and dry sand. They believed that the heat convection caused by the thermally induced pore fluid flow may affect the estimation results of the effective thermal conductivity for the saturated sand. In another study, Ghasemi-Fare and Basu (2019) found that the natural convection increased 12% the thermal performance of geothermal pipes embedded in the saturated sand. Bidarmaghz and Narsilio (2022) used a numerical model to investigate the influence of the convection on borehole heat exchanger. The results indicated that a higher fluid flow rate and permeability of ground results in better heat transfer efficiency of the boreholes (i.e., up to 43% and 63% increase, respectively). From the results of the previous studies, it can be seen that there are very few studies that quantitatively evaluate the influence of each type of convection on the performance of geothermal energy systems. Therefore, this study evaluates the influence of all three types of convection on the heat transfer performance of the EWS system, specifically the outlet fluid temperature. Furthermore, different soil types often have different hydraulic properties, so the influence of convection types on each soil type is also different. This study uses the difference groundwater flow velocity level to represent the difference three typical soil types (sand, silty sand, and clay) for the study. 3D numerical models were built to simulate the heat transfer process when operating the EWS. The 3D model simulates the pipeline and evaluates the influence of convection types on the outlet fluid temperature. The model was validated with in situ TRT experiments using a U-type heat exchanger buried in a concrete cube of 5 × 3 × 2 m.

2 STUDY PROGRAM

2.1 *Thermal performance analysis*

The heat exchange in the energy wall includes heat conduction and heat convection of the ground domain (porous medium) and heat convection of the circulating fluid in the pipe. For the ground domain, the heat transfer equation can be described as follows:

$$(\rho C_P)_{pm}\frac{\partial T}{\partial t} + (\rho C_P)_w(\vec{u}\nabla T) = k_{pm}(\nabla^2 T) \quad (1)$$

where T is temperature, t is time, $(\rho C_p)_w$ is the volumetric heat capacity of water. In addition, $(\rho C_p)_{pm}$ and k_{pm} is the specific heat capacity and thermal conductivity of saturated porous medium, which is calculated following Eq. (2) and Eq. (3), respectively.

$$(\rho C_P)_{pm} = \varepsilon(\rho C_P)_w + (1-\varepsilon)(\rho C_P)_s \quad (2)$$

$$k_{pm} = \varepsilon k_w + (1-\varepsilon)k_s \quad (3)$$

where k_w and k_s is the thermal conductivity of water and solid, respectively.

The Darcy-Brinkman-Forchheimer momentum equation presented for the convection of groundwater flow within the porous medium can be expressed as follows.

$$\begin{aligned}\frac{\rho_w}{\varepsilon}\left(\frac{\partial \vec{u}}{\partial t} + (\vec{u}.\nabla)\frac{\vec{u}}{\varepsilon}\right) &= -\nabla P.I \\ &+ \nabla\left[\frac{\mu}{\varepsilon}\left\{\nabla\vec{u} + (\nabla\vec{u})^T + \frac{2}{3}\nabla.\vec{u}I\right\}\right] \\ &- \frac{\mu}{K}\vec{u} - \frac{C_F\rho_w\varepsilon}{K^{1/2}}|\vec{u}|\vec{u} + F_B\end{aligned} \quad (4)$$

where C_F is Forchheimer coefficient, P is pressure field, K is permeability of the ground, μ and ρ_w are dynamic viscosity of the pore water and density, respectively. In addition, F_B represents the buoyancy force created by the density change caused by the temperature change of the water during the operation of the energy wall. It can be expressed as follows.

$$F_B = [0; 0; p_w g] \quad (5)$$

where the density of water, ρ_w, can be expressed as a function of the initial density value ρ_{w0} (at the temperature of T_0), the temperature difference, and the volumetric thermal expansion coefficient of water (β) as follows Eq. (6).

$$\rho_w = \rho_{w0}\{1 - \beta(T - T_0)\} \quad (6)$$

Regarding the heat convection of the circulating fluid in the pipe, the heat exchange equation can be expressed as follows:

$$\begin{aligned}\rho_f A_p C_p\frac{\partial T_f}{\partial t} + \rho_f A_p C_p u\cdot\nabla T_f &= \nabla\cdot(\lambda_f A_p \nabla T_f) \\ &+ \frac{1}{2}f_D\frac{\rho A_p}{2d_h}|u|u^2 + Q + Q_{wall}\end{aligned} \quad (7)$$

In the above, $(1/2)f_D(\rho A_p/2d_h)|u|u^2$ is the friction heat dissipated caused by the fluid's viscosity, d_h is the mean hydraulic diameter (m), u represents the tangential fluid velocity (m s^{-1}), and f_D is the coefficient of friction, which can be determined using Churchill's friction model (Eqs. (8), (9, (10)).

$$f_D = 8\left[\left(\frac{8}{Re}\right)^{12} + (C_A + C_B)^{-1.5}\right]^{1/12} \quad (8)$$

$$C_A = \left[-2.457\ln\left(\left(\frac{7}{Re}\right)^{0.9} + 0.27\left(\frac{e_s}{d_h}\right)\right)\right]^{16} \quad (9)$$

$$C_B = \left(\frac{37530}{Re}\right)^{16} \quad (10)$$

In addition, Q_{wall} represents the heat transfer externally between the surrounding soils and the pipe wall, which can be determined as following Eq (11):

$$Q_{wall} = (hZ)_{eff}(T_p - T_f) \quad (11)$$

where the effective hZ (W/(mK)) of a circular tube is determined as following Eq. (12):

$$(hZ)_{eff} = \frac{2\pi}{\frac{1}{r_0 h_{int}} + \sum_{n=1}^{N}\frac{\ln\left(\frac{r_n}{r_n - 1}\right)}{\lambda_n}} \quad (12)$$

$$h_{int} = Nu\frac{\lambda_f}{d_h} \quad (13)$$

In the above, r_N and r_0 denote the outer and inner radii of the pipe wall (m), respectively, and r_n (ranges from r_0 to r_N) is the radius of the n^{th} wall's radius (m). In addition, λ_n is the n^{th} wall's thermal conductivity (W/(mK)), and h_{int} represents the internal film heat transfer coefficients of the pipe wall, d_h represents the tube's hydraulic diameter. For the laminar flow in a circular pipe cross section, *Nu* can be determined as equal to 3.66. Regarding turbulent pipe flow, *Nu* depends on Prandtl number Pr, and can be calculated using Gnielinski equation, as following Eq. (14):

$$Nu = \frac{\left(\frac{f_D}{8}\right)(Re - 1000)Pr}{1 + 12.7\left(\frac{f_D}{8}\right)^{0.5}(Pr^{2/3} - 1)} \quad (14)$$

Table 1. Input parameter for the numerical model.

Domain	Parameter	Value	Unit
Global parameters	Inlet fluid temperature	60	°C
	Flow rate of circulating fluid	8	l/min
	Dimension of domain	50×60×70	m
	Thickness of concrete wall	0.78	m
Ground	Thermal conductivity of ground (Sand/Silt/Clay)	1.5	W/(mK)
	Specific heat capacity of ground (Sand/Silt/Clay)	1615	J/(kgK)
	Density of ground (Sand/Silt/Clay)	2066	kg/m^3
	Porosity	0.3	-
Concrete	Thermal conductivity of concrete	2.5	W/(mK)
	Specific heat capacity of concrete	1100	J/(kgK)

	Density of concrete	2500	kg/m^3
	Porosity	0.05	-
Pipe (Polybutylene)	Thermal conductivity	0.38	W/(mK)
	Specific heat capacity	525	J/(kgK)
	Density of PB pipe (TRT pipe)	955	kg/m^3
Fluid	Thermal conductivity of circulating fluid (water)	0.6	W/(mK)
	Specific heat capacity of circulating fluid (water)	4180	J/(kgK)
	Density of circulating fluid (water)	1000	kg/m^3
	Dynamic viscosity of circulating fluid (water)	0.001	Pa.s
	Fluid volumetric thermal expansion	10^{-6}	1/K

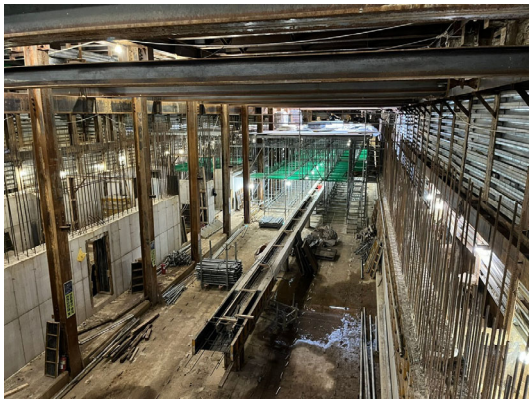

Figure 1. An actual subway station constructed at Gwangju, South Korea

An actual subway station constructed in Gwangju, South Korea, was employed for the numerical model (Figure 1). The height and the width of the subway station are 5.6 and 8.45 m, respectively. A concrete wall with a thickness of 700 mm was used. It should be noted that an energy wall unit with a length of 20 m was modeled to consider real construction stage and reduce the analysis time.

Figure 2 shows the numerical model of the energy wall system. The size of the ground domain is 50 × 60 × 70 m (height × length × width), and is divided into three layers, with heights of 6 m, 34 m, and 10 m, respectively. The middle layer is considered as the aquifer where convection occurs. To evaluate the influence of soil hydraulic properties on the impact of groundwater convection, three typical soil types, sand, silt, and clay, are considered as porous media in this aquifer layer. The energy wall (concrete wall) is placed at a depth of 12 m from the ground surface, with dimensions of 10 × 60 × 12 m (height × length × width), and the width of the concrete wall is 0.78 m. The concrete used has a density of 2500 kg/m^3, and a thermal conductivity of 2.5 W/(mK). Different from the simplified 2D model of the heat source as a line heat source, the 3D model simulates the heat transfer process of the fluid in the pipe to quantitatively evaluate the influence of underground flow in the soil on the outlet temperature of the energy wall. Regarding the pipeline, the pipe material used is Polybutylene pipe, with high durability and flexibility. The pipe is installed in a vertical U-shape, with a distance between 2 pipes of 15 cm. The inner and outer diameters of the pipe are 1.6 cm and 2.0 cm, respectively. The total length of the pipe is 552 m to simulate an actual size of 1 energy wall unit (20 m long). To evaluate the influence of inlet fluid temperature on outlet fluid temperature, the inlet fluid temperature of 60 ºC was selected. The flow rate of circulating fluid was set as constant as 8 l/min.

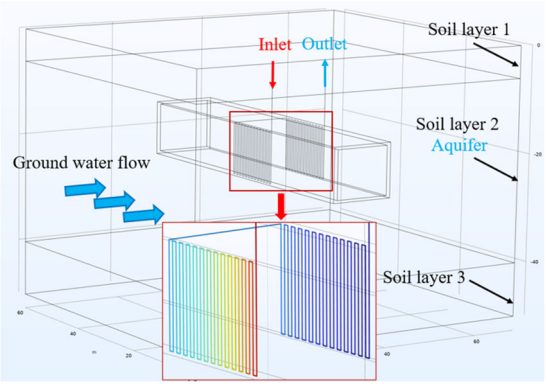

Figure 2. COMSOL Multiphysics based numerical model of energy wall system

2.2 *Validation results*

The in-situ thermal response test was conducted on the concrete trench (Figure 3). A 5 m length U-type heat exchanger was installed at a depth of 2 m. The dimension of the TRT trench is 5 × 3 × 2 m, thus a total volume of 30 m^3 of fresh concrete was used. The thermal properties of the concrete were measured using an M1 device at the laboratory (Kapton hot disk sensor type, ISO), while the thermal properties of the soil were measured at the site using a KD2 pro (needle type, ASTM).

Figure 3. TRT trench preparation

Table 2 lists the equipment used for the TRT. The testing time of TRT was more than 50 h, with the constant flow rate of about 9.58 l/min. 2 RTD sensors were used to measure the inlet and outlet fluid temperature, and another 4 RTD sensors were installed in the soil to measure the ground temperature change during the TRT. The fluid temperature, flow rate of fluid, and the thermal properties of concrete and surrounding soil were employed as the input parameters for the numerical model.

Table 2. Lists of equipment used for the TRT

Devices	Description	Quantity

Temperature sensor	Measurement range (0–150 °C), (PT 100, Class A, four wire)	5
Heater	Maximum capacity of 5 kW	1
Flowmeter	Accuracy of 0.1 l/min, measurement range: 0.03–15 m/s	1
Water tank	20 L	1
Data acquisition system	Four wire scanning, 22 channel Multiplexer, DAQM901A	1
Data logger	Keysight DAQ970A	1

3 RESULTS AND DISCUSSION

3.1 *Validation results of numerical model*

Figure 4 shows the fluid temperature and the surrounding soil temperature of in-situ experimental results and numerical analysis. The relative error was calculated following Eq. (15) and presented in Figure 4(b). The difference between numerical and experimental results was lower than 2.5% for outlet fluid temperature and indicated that the accuracy of the numerical model.

$$RE(\%) = \sqrt{\frac{\sum_i (T_i^{Numerical} - T_i^{TRT})^2}{\sum_i (T_i^{TRT})^2}} \times 100 \qquad (15)$$

where RE is the relative error of the fluid temperature, $T_i^{Numerical}$, and T_i^{TRT} is the outlet fluid temperature of the numerical and experimental measurement (TRT), respectively.

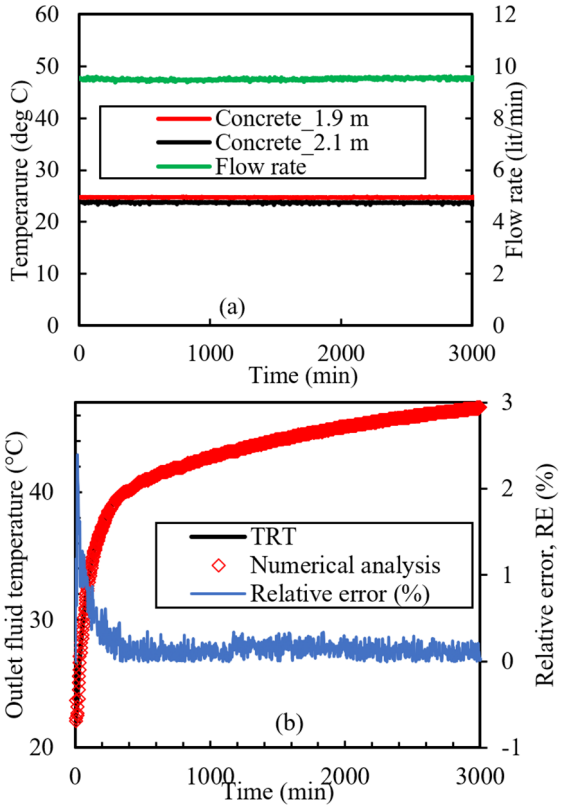

Figure 4. The TRT and numerical analysis results (a) flow rate and measured soil temperature, (b) relative error between numerical model and experimental results (TRT).

3.2 *Effect of convection on flow vector and temperature of surrounding soils*

To evaluate the effect of convection on the thermal performance of the energy wall, the pipeline was modelled, and therefore, the heat transfer in a pipe was added as for 3D modelling of the energy wall. The inlet fluid temperature was set as constant at 60 °C. The left side of the energy wall is the inlet fluid, and the outlet fluid is on the right side (Figure 2).

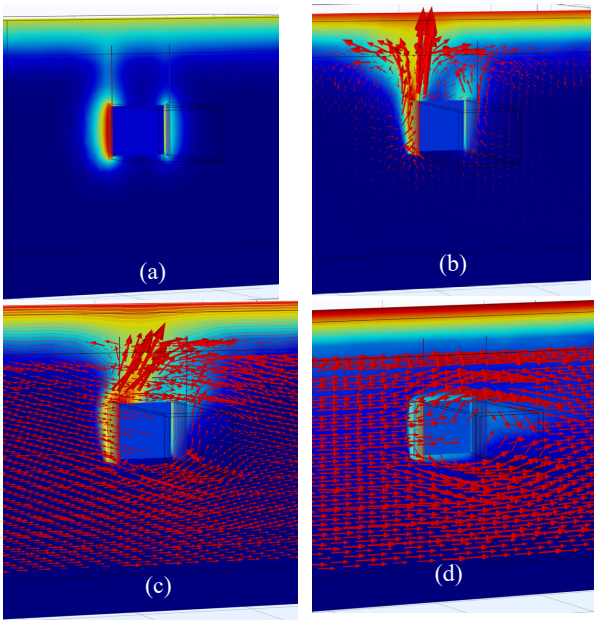

Figure 5. 3D model results–flow vector and ground temperature of: (a) no convection, (b) natural convection (u = 0.03 m/year), (c) mixed convection (u = 3 m/year), and (d) forced convection (u = 300 m/year).

At a low GW flow velocity of 10^{-8} m/s (about 0.3 m/year), the natural convection mainly occurred, and was clearly observed at the inlet side, rather than the outlet side of the EWS. In addition, the natural convection caused by the buoyancy force shifts the maximum ground temperature point 5-10 m to the top of the EWS. Consequently, the affected zone was shifted from a depth of 15–25 m to 5–20 m (Figure 6(b)). When the GW velocity increases to 10^{-6} m/s (30 m/year), the mix between the natural convection and forced convection was observed in the inlet side of the EWS. The ground temperature in the case of mixed convection was slightly lower than that of natural convection. However, at the high GW velocity of 10^{-5} m/s (about 300 m/year), the maximum of the soil temperature was dramatically decreased to about 21 °C. In this scenario, the forced convection overcame the effect of the natural convection; therefore, only the thermally induced pore water flow from left to right was observed. Another difference between the pipeline embedded model (3D) and the heat source model (2D) is the difference in the ground temperature alongside the EWS. As shown in Figure 7, the temperature difference alongside the ground was 10 °C for the inlet side (Figure 7(a)) and 6 °C for the outlet side (Figure 7(b)).

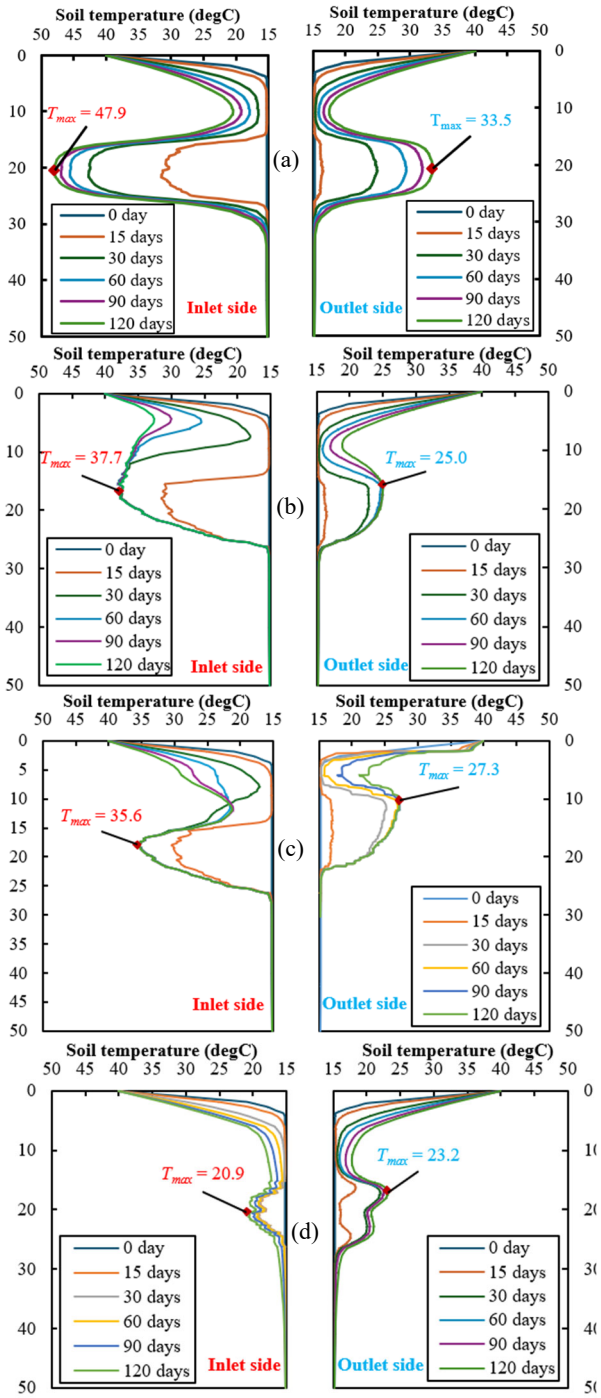

Figure 6. Effect of the convection on soil temperature cause by the thermally induced pore water flow in pipeline coupling model (3D): (a) no convection, (b) natural convection ($v = 10^{-8}$ m/year), (c) mixed convection ($v = 10^{-7}$ m/year), and (d) forced convection ($v = 10^{-5}$ m/year).

3.3 *Effect of convection on fluid temperature and heat transfer performance*

The convection has a significant positive effect on the heat exchange efficiency of the EWS. As shown in Figure 8(b) shows the outlet fluid temperature of the cooling model of EWS. When the inlet fluid temperature is set as 60 °C, the difference between the inlet and outlet fluid temperature was 20 °C for the case of only conduction, and 28 °C and 31 °C when considering the influence of natural convection and mixed convection, respectively. For the forced convection generated at the high GW velocity, the difference between inlet and outlet fluid temperature increases to 35 °C after 6 months of operation of EWS.

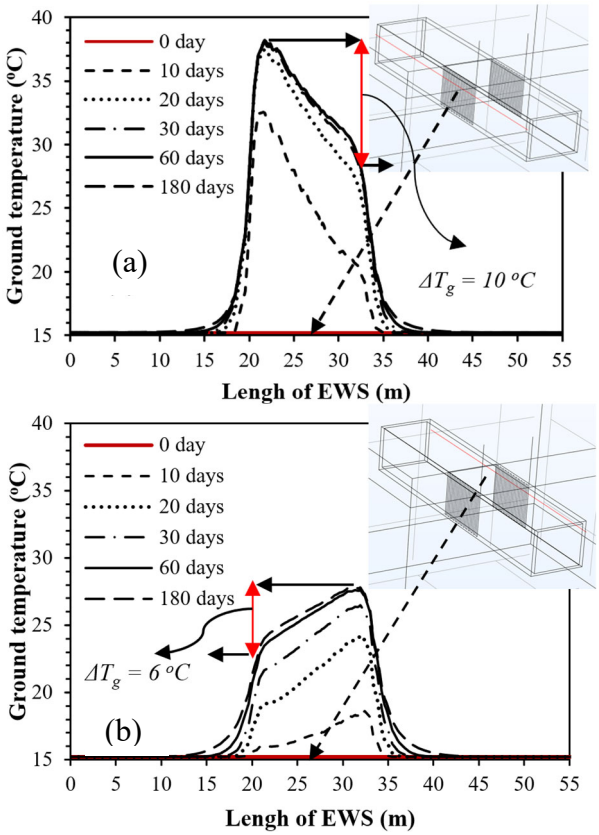

Figure 7. Effect of circulating fluid flow direction on the ground temperature: (a) Inlet side, (b) Outlet side

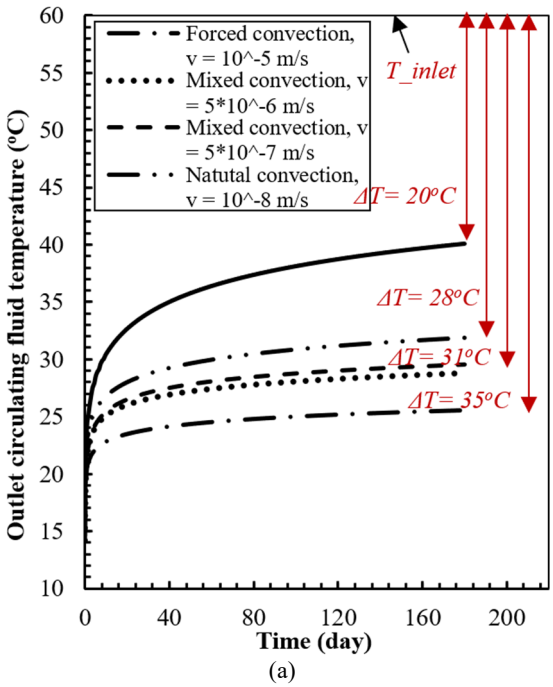

(a)

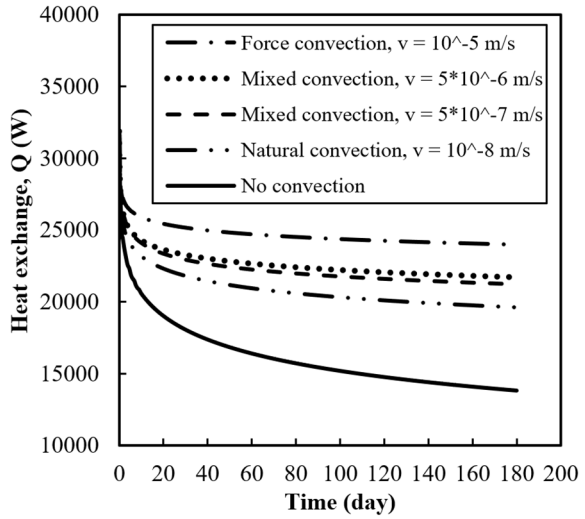

(b)

Figure 8. Effect of convection types on the (a) outlet fluid temperature (b) heat transfer performance

To quantitatively investigate the influence of convection on the efficiency of the EWS, the heat exchange, Q, was calculated as follows:

$$Q = mc(T_{fluid\_in} - T_{fluid\_out}) \quad (16)$$

where $T_{fluid\text{-}in}$ and T_{fluid_out} represent the inlet and outlet temperature of circulating fluid inside the pipe, respectively; m is the flow rate, and c is the specific heat capacity of the circulating fluid. Based on Eq. (16), the heat exchange, Q, of EWS for no convection, natural convection, mixed convection, and forced convection ($v = 5\times10^{-6}$ m/s) are 13856 W, 19609 W, 21732 W, and 23989 W, respectively (Figure 8(b)); thus, compared to no convection, the enhancement of heat exchange, Q, are 41.5% for natural convection, 56.8% mixed convection, and 73.1% for forced convection.

4 CONCLUSIONS

This study evaluates the influence of thermally induced groundwater flow on the change of temperature of the surrounding soil and outlet fluid as well as the quantitative change of the heat transfer performance of the energy wall. The important findings are as follows:

- The affected zone of soil during the operation of the energy wall strongly depended on the thermally induced groundwater flow. The natural convection moves the affected zone from the bottom to the top of the EWS, while the forced convection induces the heat following the flow direction of the groundwater flow. Therefore, the effect zone significantly differs between the left and right sides of the EWS. In addition, mixed convection generally occurs at the medium permeability of the soil (e.g., weathered granite soil) as a combination of natural convection and forced convection.
- The results revealed that groundwater velocity plays a crucial role in determining the dominant heat transfer mechanism: natural convection prevailed at velocities below 10^{-7} m/s, forced convection dominated at velocities above 5×10^{-6} m/s, and a combination of both (mixed convection) occurred between these thresholds.
- The influence of GW-induced convection on the heat transfer performance of the EWS was found to be significant. Compared to a conduction-only scenario, natural, mixed, and forced convection improved the heat exchange performance by approximately 41.5%, 56.8%, and 73.1%, respectively. Correspondingly, the outlet fluid temperature during summer operation was reduced more by 8°C, 11°C, and 15°C for natural, mixed, and forced convection, respectively, than conduction only case indicating a substantial enhancement in cooling efficiency.
- The result of this study indicated that neglecting the effect of thermally induced GW flow can result in considerable underestimation of the thermal performance and long-term efficiency of the EWS.

5 ACKNOWLEDGEMENTS

This work was supported by a Basic Research Laboratory (BRL) research grant from the National Research Foundation of Korea (NRF) (No. RS–2025-00512551).

6 REFERENCES

Bidarmaghz, A. and Narsilio, G.A., 2022. Is natural convection within an aquifer a critical phenomenon in deep borehole heat exchangers' efficiency? *Applied Thermal Engineering*, [online] 212, p.118450. https://doi.org/10.1016/J.APPLTHERMALENG.2022.118450.

Gao, B., Zhu, X., Yang, X., Yuan, Y., Yu, N. and Ni, J., 2021. Operation performance test and energy efficiency analysis of ground-source heat pump systems. *Journal of Building Engineering*, [online] 41, p.102446. https://doi.org/10.1016/J.JOBE.2021.102446.

Ghasemi-Fare, O. and Basu, P., 2018. Influences of ground saturation and thermal boundary condition on energy harvesting using geothermal piles. *Energy and Buildings*, [online] 165, pp.340–351. https://doi.org/10.1016/J.ENBUILD.2018.01.030.

Ghasemi-Fare, O. and Basu, P., 2019. Coupling heat and buoyant fluid flow for thermal performance assessment of geothermal piles. *Computers and Geotechnics*, [online] 116, p.103211. https://doi.org/10.1016/J.COMPGEO.2019.103211.

Javed, S. and Spitler, J., 2017. Accuracy of borehole thermal resistance calculation methods for grouted single U-tube ground heat exchangers. *Applied Energy*, [online] 187, pp.790–806. https://doi.org/10.1016/J.APENERGY.2016.11.079.

Kim, E., Lee, J., Jeong, Y., Hwang, Y., Lee, S. and Park, N., 2012. Performance evaluation under the actual operating condition of a vertical ground source heat pump system in a school building. *Energy and Buildings*, [online] 50, pp.1–6. https://doi.org/10.1016/J.ENBUILD.2012.02.006.

Najafian Jazi, F., Ghasemi-Fare, O. and Rockaway, T.D., 2024. Natural convection effect on heat transfer in saturated soils under the influence of confined and unconfined subsurface flow. *Applied Thermal Engineering*, [online] 237, p.121805. https://doi.org/10.1016/J.APPLTHERMALENG.2023.121805.

Sarbu, I. and Sebarchievici, C., 2014. General review of ground-source heat pump systems for heating and cooling of buildings. *Energy and Buildings*, [online] 70, pp.441–454. https://doi.org/10.1016/J.ENBUILD.2013.11.068.

Sharqawy, M.H., Badr, H.M. and Mokheimer, E.M., 2013. Investigation of buoyancy effects on heat transfer between a vertical borehole heat exchanger and the ground. *Geothermics*, [online] 48, pp.52–59. https://doi.org/10.1016/J.GEOTHERMICS.2013.04.003.

Spitler, J.D., Javed, S. and Ramstad, R.K., 2016. Natural convection in groundwater-filled boreholes used as ground heat exchangers. *Applied Energy*, [online] 164, pp.352–365. https://doi.org/10.1016/J.APENERGY.2015.11.041.

Tamizdoust, M.M. and Ghasemi-Fare, O., 2020. A fully coupled thermo-poro-mechanical finite element analysis to predict the thermal pressurization and thermally induced pore fluid flow in soil media. *Computers and Geotechnics*, [online] 117, p.103250. https://doi.org/10.1016/J.COMPGEO.2019.103250.

Zhao, J., Wang, H., Li, X. and Dai, C., 2008. Experimental investigation and theoretical model of heat transfer of saturated soil around coaxial ground coupled heat exchanger. *Applied Thermal Engineering*, [online] 28(2–3), pp.116–125. https://doi.org/10.1016/J.APPLTHERMALENG.2007.03.033.